PROGRESS TOWARDS INVESTIGATION OF THE IMPACT OF TARGETED INHIBITION OF POTENTIAL DNA-DAMAGE RESPONSE REGULATION OF TRANSLATION IN IRRADIATED NON-SMALL CELL LUNG CANCER CELL LINES

by

Eleanor M. Johnston

BS, University of Pittsburgh, 2014

Submitted to the Graduate Faculty of
School of Medicine in partial fulfillment
of the requirements for the degree of
Master's of Science

University of Pittsburgh
2018

UNIVERITY OF PITTSBURGH

SCHOOL OF MEDICINE

This thesis was presented

by

Eleanor M. Johnston

It was defended on

August 3, 2018

and approved by

Guillermo Romero, Associate Professor, Department of Pharmacology and Chemical Biology, Vice Director of Molecular Pharmacology Graduate Program

Roderick O'Sullivan, Assistant Professor, Department of Pharmacology and Chemical Biology

Thesis Advisor: Christopher Bakkenist, Associate Professor and Vice Chair of Basic Science, Department of Radiation Oncology

PROGRESS TOWARDS INVESTIGATION OF THE IMPACT OF TARGETED INHIBITION OF POTENTIAL DNA-DAMAGE RESPONSE REGULATION OF TRANSLATION IN IRRADIATED NON-SMALL CELL LUNG CANCER CELL LINES

Eleanor M. Johnston, M.S.

University of Pittsburgh, 2018

Lung cancer has a 5-year survival rate of 17% with current standard-of-care radiation and chemotherapies (1,2,4,8,9). Immune escape contributes to poor tumor clearance driving the development of therapies that promote anti-tumor immune responses (29-33). The cytotoxic T-lymphocyte response distinguishes cancerous cells by the presentation of mutated endogenous antigens on MHC-1 molecules (26,29-33). Radiation therapy has been shown to increase MHC-1 antigen presentation (22-23,30). It has been proposed that DNA-damage response signaling inhibits translation during radiation induced cell recovery resulting in a post-repair spike in translation and MHC-1 presentation (22-23,30). We hypothesize that ATM and ATR inhibition will disrupt the negative regulation of translation post-radiation to impact the rate of MHC-1 presentation. Increasing antigen presentation before cell recovery from radiation damage may increase the magnitude of mutant antigens to stimulate anti-tumor CD8+ T-cell activation.

This investigation attempted to monitor the impact of DNA-damage response inhibition on translation and subsequent MHC-1 presentation post-radiation at two levels. First, fluctuations in the intracellular peptide pool available for MHC-1 antigen loading was measured via the activity of Transporter associated with Antigen Processing (TAP) responsible for shuttling cytosolic peptides into the ER for MHC-1 antigen loading (20-2226). Fluorescence Recovery After Photobleaching (FRAP) of TAP1-mNeonGreen was used to calculate the lateral diffusion of TAP within the ER membrane as diffusion is inversely correlated to TAP activity. Second, MHC-1 cell surface presentation was measured via flow cytometry.

ACKNOWLEDGEMENTS

I offer my sincere gratitude to my thesis advisor, Chris Bakkenist, for the opportunity to pursue my graduate career in his laboratory. Although my time was short, I appreciate the welcome, guidance, and support during my journey. I would like to extend my thanks to Sandy, Tatiana, Frank, Norie, Katie, Pooja, and Jeff for a joyful and stimulating lab environment. The assistance and encouragement from the lab, both scientific and not, sustained me during my time here.

Many thanks to the staff within the Interdisciplinary Biomedical Graduate Program and Molecular Pharmacology Graduate Program for the administrative support and the Center for Biologic Imaging for their expertise. Finally, I would like to thank my thesis committee for the scientific advice and flexibility during my tenure in the program.

TABLE OF CONTENTS

LIST OF FIGURES

LIST OF TABLES

1.0 INTRODUCTION

1.1 LUNG CANCER THERAPEUTICS

In 2017, lung and bronchial cancer was the leading cause of cancer related death for both sexes (27% male, 25% male) in the United States, more than colorectal, prostate, and breast cancer combined (1,7,8). Approximately 85% of lung cancer patients have non-small cell lung cancer (NSCLC) (1,2,4,7,8,9). With current standard-of-care therapies, lung cancer has the second lowest five-year survival rate at approximately 17% highlighting the need for improved therapeutics (1,2,4,7,8,9). Early detected stage I and II lung cancer patients are eligible for surgical resection and may receive adjuvant therapy to improve tumor clearance (2,4,8). The majority of patients are diagnosed with advanced (stage III) or metastatic (stage IV) cancer and are ineligible for surgery as it would be too invasive. Treatment options for stage III and IV patients include radiation, chemotherapy, targeted therapy, immunotherapy, or a combination thereof (2,4,8).

Standard-of-care cancer therapeutics attempt to target one or more of the 'Hallmarks of Cancer' which include six accepted functional capabilities and two enabling characteristics. The functional characteristics are sustained cellular proliferation, evasion of growth suppressors, resisting cell death, replicative immortality, angiogenesis, and an activate invasive or metastatic phenotype (19). Genome instability and tumor promoting inflammatory condition are considered enabling characteristics, or rather the environmental and genomic basis for the induction of the six functional characteristics through the mutation or dysregulation of cellular processes (19). Dysregulation of cellular energetics and immune evasion are recognized as emerging 'hallmarks of cancer' (19).

Targeted therapies are small molecule compounds that have been identified and designed to target specific mutated, upregulated, or downregulated proteins in pathways involved in proliferation, evasion of growth suppressors, resisting cell death, angiogenesis, and metastasis. In NSCLC, the most commonly (10-35% of patients) mutated or upregulated growth stimulating pathway is the EGFR pathway (2,4,7,8). Small molecule ATP competitive inhibitors erlotinib, gefitinib, and afatinib target active site of the EGF receptor tyrosine kinase to inhibit tumor cell proliferation (4,2,7,8). Kinase inhibitors crizotinib, certitinib, and alectinib, target the ALK active site in the EML4-ALK translocation mutant implicated in malignant transformation in lung cancer (2,4,7,8,11). BRAF kinase inhibitors dabrafenib and trametinib target the BRAF growth stimulating pathways (2,4,7,8). Anti-angiogenesis drugs, bevacizumab or ramucirumab, inhibit the VEGF signaling for new blood vessel formation in tumors (2,4,7,8). Targeted therapies selected to combat specific mutation profiles produce significant patient response; however, often patients experience a resurgence of more aggressive tumors containing resistance mutations that decrease targeted kinase inhibitor efficacy or upregulate compensatory growth pathways (2,4,7,810). The development of resistance mutations is the constant uphill battle for pharmacologic development of new generations of kinase inhibitors, improving patient molecular screening, and clinical treatment.

Immunotherapies are an emerging branch of targeted therapies which inhibit tumor immune evasion by disrupting the signaling of immune inactivating signals. Lung cancer patients have demonstrated high success with emerging immunotherapies nivolumab and prembrolizumab which target the PD1/PD-L1 immune checkpoint which inhibits tumor cell activation of the cytotoxic-T lymphocytes (2,4,7,8,30-33). Patients with increased PD-L1 surface expression respond well and as these therapies target a receptor interaction, the development of resistance mutations is low. However, patients without PD-L1 expression profile are not as responsive reducing the effective population for this particular immunotherapy (30-33).

Considering the disadvantages of targeted therapy, chemotherapy remains a standard-of-care for lung cancer patients (4,2,7,8). DNA damaging agents which intercalate into DNA (cisplatin, carboplatin) or inhibit topoisomerases (irinotecan, etoposide) induce the accumulation of lethal DNA lesions that stimulate cell death (2,4,7,8). Anti-metabolites (pemetrexed, gemcitabine) inhibit the generation of nucleic acids for DNA synthesis halting cell proliferation

(2,4,7,8). Anti-microtubules (docetaxel, paclitaxel) inhibit cytoskeletal microtubule function preventing cell division and proliferation. Chemotherapy is administered as the primary treatment, adjuvant to surgery and radiation, or as a combination of chemotherapy (2,4,7,8). The main advantage to chemotherapy is that consistent patient responses can be achieved regardless of patient molecular profiles. However, these drugs have severe side effects due to the toxicity for normal tissues which significantly decrease the patient's quality of life.

Radiation therapy, another standard treatment for lung cancer patients, utilizes the intersection of multiple high-energy particles or x-rays expose tumors to lethal doses of radiation while exposing surrounding tissues to sublethal doses (2,4,7,8). Radiation exposure causes direct and indirect (reactive radicals from radiolysis) damage to proteins, DNA, and cell organelles stimulating cell death. Radiation therapy does not rely on blood supply and therefore does not produce systemic toxicities, which is a major advantage. However, radiation therapy is not suitable for widespread cancers, and thus limited in benefit for advanced metastatic cancers. Often radiation therapy is combined with a chemical therapy to improve tumor clearance (2,4,7,8).

Research to improve standard-of-care therapies include combining DNA damaging agents with targeted DNA-damage response inhibitors (5, 12-18,35-47). Targeted DNA-damage response inhibition takes advantage of the genomic instability inherent in cancer to induce the accumulation of lethal amounts of DNA damage to stimulate cell death by inhibiting the signaling pathways that regulate DNA repair and cell cycle arrest. The simultaneous generation of DNA damage and inhibition of DNA-damage response pathways increases the accumulation and propagation of DNA damage through the cell cycle and ultimately induces cell death (12-18,35-47). The combination of these therapies can increase the therapeutic window to generate better patient responses with decreased side effects. The investigation described in this thesis involves the study of how combing radiation with targeted DNA-damage response inhibition may also combat another 'hallmark of cancer' by impacting expression of activating immune response receptors.

1.2 TARGETING THE DNA DAMAGE RESPONSE IN CANCER

The DNA-damage response is a network of enzymatic pathways that work in concert to detect, signal the presence of, and direct the repair of DNA lesions (12-18,35-47). Deficiencies in the DNA-damage response results in sensitivity to DNA damaging agents and are the cause of several human diseases (12-18,36,41-50). Ataxia telangiectasia mutated kinase (ATM) and Ataxia telangiectasia mutated-related kinase (ATR) are apical signaling kinases of the DNA-damage response (**Figure 1 and 2**). ATM and ATR are recruited to double-strand breaks (DSB) and RPA-coated ssDNA, respectively. As signaling kinases, ATM and ATR phosphorylate a broad, overlapping spectrum of substrates to modulate several cellular processes including DNA replication, DNA repair, transcription, translation, cell cycle progression, apoptosis, and senescence (**Figure 1 and 2**) (12-18).

DNA damage induced by radiation and DNA damaging chemotherapy activate both ATM and ATR (12-18,35-47). Double-strand breaks from radiation induce the activation of ATM or DNA-PK kinases to regulate homologous recombination (HR) or non-homologous end joining (NHEJ) DNA repair pathways, respectively (**Figure 1**) (12-18). Similarly, alkylating agents or crosslinking agents like Cisplatin that stall the replication fork progression generate RPA coated ssDNA which recruits and activates ATR kinase to regulate the replisome stability, origin firing, and repair (**Figure 1**) (12-18). In addition to regulating DNA repair, the DNA damage response kinases regulate cell cycle progression, apoptosis, and senescence. Inhibition of ATM or ATR leads to deficient G1/S, S, or G2/M checkpoints (**Figure 2**) (12-18,35-47). This causes DNA damage to be propagated through the cell cycle simulating replicative and/or mitotic catastrophe and cell death (12-18,35-47). Therefore, inhibiting both DNA repair and checkpoint signaling lowers the dose of damaging agents necessary to induce death by providing an easier environment for the accumulation of lethal amounts of DNA damage.

Loss of ATM (ataxia telangiectasia mutated) in ataxia telangiectasia patients, and transient pharmacologic inhibition of ATM has been documented to sensitizes cells to radiation (35,37,40,41-46). ATR inhibitors have been observed to be well tolerated *in vivo* and sensitize lung cancer cells to cisplatin and IR (35-40). Due to the compensatory nature of the DNA-damage response, deficiencies in one pathway often provides sensitivity to inhibition of other pathways.

For example, ATM loss in cancer has been associated with increased ATR activity which provides a 'synthetic lethal' environment for ATR inhibition (35,37,40,41-46). The Bakkensit lab has published that ATR inhibition synergizes with cisplatin to kill ATM deficient lung cancer cells and xenografts (35). DNA-damage response inhibition potentiates DNA damage from radiation and chemotherapy agents like cisplatin, gemcitabine, or irinotecan through the cell cycle checkpoints to induce mitotic catastrophe thereby decreasing the IC50, lowering dosing concentration, and providing relief from toxic side effects associated with these standard-of-care (35,37,40,41-46). The DNA-damage response has been suggested to contribute to translation regulation especially post radiation (23,24). Translation levels modulate immune receptor expression and presentation. Inhibition of the DNA-damage response in combination with radiation; therefore, may provide a means to impact immune responses post-radiation therapy.

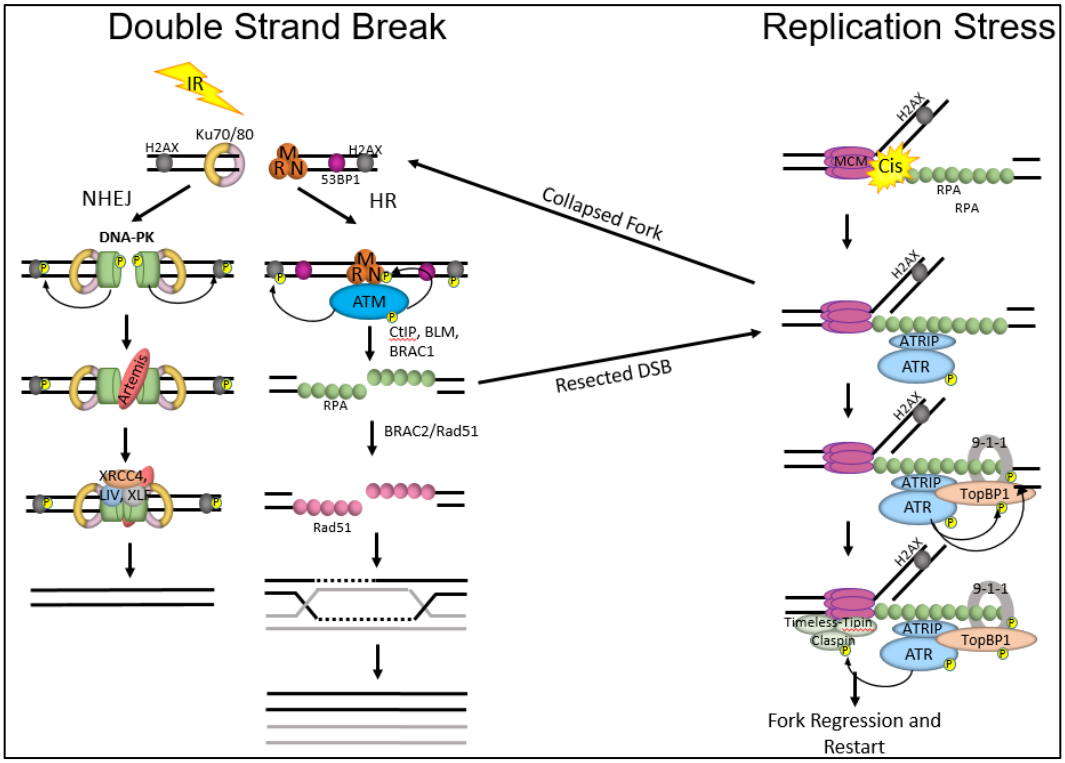

Figure 1: DNA-Damage Response Activation and Regulation of DNA Repair
DNA damage response signaling kinases, ATM and ATR, are activated at DNA double-strand breaks and single-stranded DNA associated with stalled replication forks and resected double-strand breaks, respectively. Radiation induced double strand breaks stimulate the activation of ATM or DNA-PK kinases to regulate HR or NHEJ DNA repair pathways, respectively. Similarly, alkylating agents or crosslinking agents like Cisplatin that stall the replication fork progression generate RPA coated ssDNA which recruits and activate ATR kinase to regulate the replisome stability, origin firing, and repair. Inhibition of ATM and ATR leads to the accumulation of DNA damage.

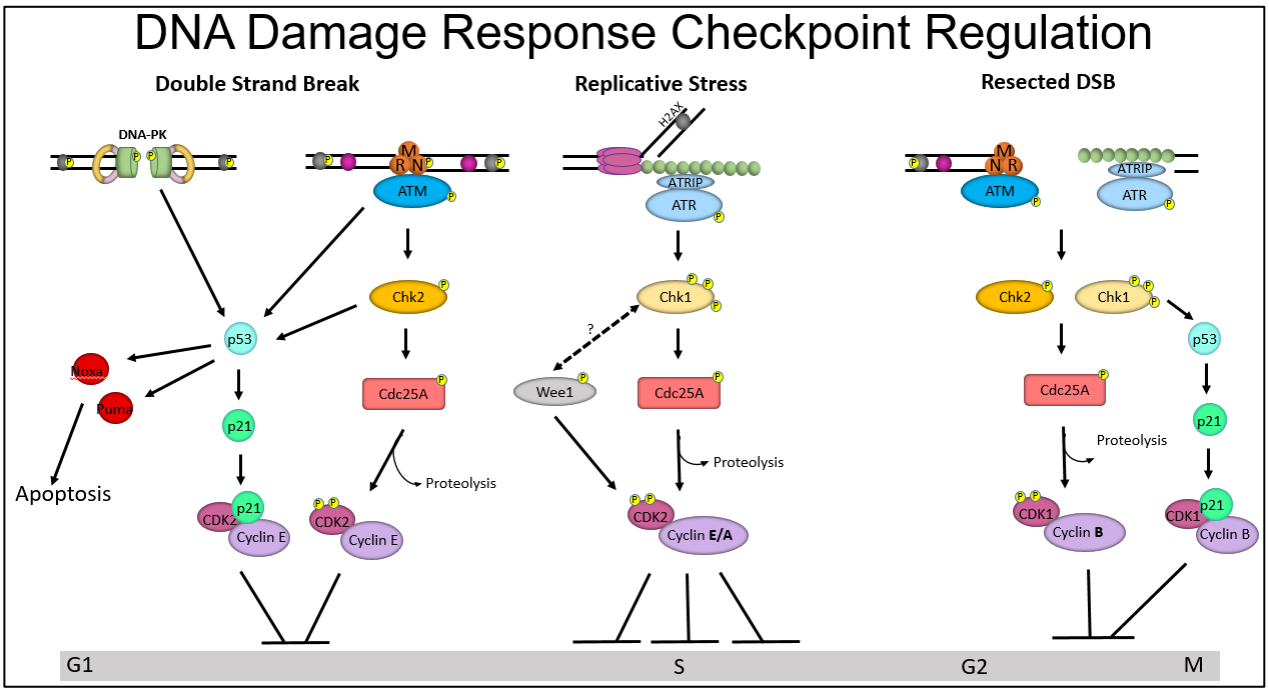

Figure 2: DNA-Damage Response Cell-Cycle Checkpoint Regulation
The DNA-damage response kinases regulate cell cycle progression, apoptosis, and senescence. Inhibition of ATM or ATR leads to deficient G1/S, S, or G2/M checkpoints. This causes the damage to be propagated through the cell cycle simulating replicative and/or mitotic catastrophe and cell death. Cdc25A is phosphatase that dephosphorylates CDK2 allowing cell cycle progression. Phosphorylation by Chk1 or Chk2 stimulates Cdc25A degradation. allowing stabilization of CDKs and cell cycle arrest or senescence. ATM/Chk2 phosphorylation of p53 leads to apoptosis or cell cycle arrest.

1.3 THE ROLE OF MHC-1 CELL SURFACE PRESENTATION IN TUMOUR CELL RECOGNITION

Major histocompatibility complex class one (MHC-1) molecules present cytosolic and nuclear protein fragments present within the cell at the cell surface (27-29). CD8+ T cells sample the presented MHC-1 antigen landscape to distinguish ‘self’ and ‘non-self’ antigens (27-30). In the event of recognition of ‘non-self’ antigen presentation, the cytotoxic T lymphocytic response is activated and leads to the clearance of the compromised cell (27-29). Within the context of cancer, presentation of antigens containing mutations stemming from the inherent genome instability or improper peptide ligations called ‘neo-antigens’ can trigger the cytotoxic T lymphocyte response against tumor cells (27, 30). Conversely, immune evasion is one of the hallmarks of cancer where tumor cells down regulate MHC-1 by increasing degradation or by increasing immune inactivating stimuli (e.g. PD-L1)(18,31-34). Current immunotherapy initiatives that target immune

deactivating receptors and have proven to be successful in NSCLC suggesting that treatment options that increase immune activating stimuli may improve tumor clearance (31-34). Similarly, increasing the prevalence of 'neo-antigen' presentation has been proposed as a method to stimulate anti-tumor immune responses (30-34).

MHC-1 cell surface presentation is regulated by the concentration of suitable peptides for loading as most MHC-1 molecules are degraded by ER-associated protein degradation systems (ERAD) without antigen loading (27-29). Proteasomal degradation of existing, nascent, or defective proteins provides the intracellular peptide pool for antigen presentation (27-29). Peptides are transported into the ER via transporter associated with antigen processing (TAP) and are trimmed in ER lumen by ERAAP before loading by the peptide loading complex (21-23,27). The MHC-1 peptide loading complex is formed by the interaction of active TAP, unfolded MHC-1, and chaperone proteins tapasin, calreticulin, and ERp57 (27-29). Once loaded with a peptide, the -chaperones release MHC-1 to pass through the ER quality control checks to pass through the golgi trafficking system to the cell surface (27-29).

Defective ribosomal products (or DRiPs) from defective transcription, translation, splicing, or failed complex assembly are degraded immediately by the proteasome to prevent aggregate formation. The immediate degradation of a fraction of newly synthesized proteins couples translation to MHC-1 presentation. Therefore, regulation of translation impacts the generation of an intracellular peptide pool for antigens. Viral infection, IFNgamma signaling, microRNA expression, and ionizing radiation exposure alter the antigen landscape by altering the amount and type of proteins being synthesized (23,24,27). Reits et al. has observed a dose dependent increase in MHC-1 presentation over several days post radiation exposure (23). The observed radiation induced increase in MHC-1 presentation was in part regulated by mTOR cap-dependent translation (21-24). This suggests that regulation of translation post-radiation can impact MHC-1 exposure. Radiation induced ATM signaling through mTOR has been observed to alter translation in transformed cell lines (24). Increasing the rate of MHC-1 expression post-radiation exposure may potentially increase the amount of defective or mutated antigens to be expressed on the cell surface. For cancer therapeutics this may present an avenue for improving immune clearance of irradiate tumor cells.

1.4 REGULATION OF CAP-DEPENDENT TRANSLATION POST-RADIATION

Cap-dependent translation is responsible for the majority of protein synthesis. The translation initiation complex forms when eukaryotic translation initiation factor 4F (eIF4F) binds the 5' cap of the mRNA and recruits eIF4G and eIF4A (**Figure3**) (25,26). The binding of eIF4F is regulated by inhibitory 4E-binind protein 1 (4E-BP1) (25,26). Phosphorylation of 4E-BP1 induces disassociation from eIF4F allowing it to bind the 5' cap of the mRNA (25,26). eIF4A is an RNA helicase that removes secondary structures prior to translation (**Figure3**). The binding of regulatory factor eIF4B enhances eIF4A activity. Phosphorylation of eIF4B increases the association of eIF4B and eIF4A increasing eIF4A helicase activity (**Figure3**) (25,26). eIF4G provides the molecular scaffolding for assembly of the 40s ribosomal subunit to the mRNA-eIF4F imitation complex (eIF4F, eIF4A- eIF4B, eIF4G) (25,26). Phosphorylation of eIF4G increases eIF4G binding to the eIF4F initiation complex. The phosphotransferase activity of mTORC1 (mTOR, raptor, and LST8) regulates translation initiation by phosphorylating 4E-BP1 and the 40S ribosomal protein S6 kinases (S6Ks) (25,26)..

Braustein et al. (2009) observed that post-radiation the DNA-damage response signaling through the p53 pathway in transformed cells. Activation of the p53, the induction of Senestrin 1/2 proteins, and activation of AMP kinase lead to the inhibition of mTOR (24). Inactive mTOR impedes the inactivation of 4E-BP1 and the phosphorylation of 40S ribosomal S6Ks decreasing cap-dependent translation. During cellular recovery, activation of the DNA-damage response ATM-p53 axis maintained cap-dependent translation inhibition (24). In non-transformed cells, radiation activates ERK1/2 resulting in transient mTOR regulated cap-dependent translation of DNA repair proteins and cell survival proteins (24). The role for ATR signaling in translation regulation was not elucidated. Reits et al. observed increased mTOR regulated translation and MHC-1 surface presentation post-radiation highlighting the potential for an DNA-damage response dependent impact on MHC-1 presentation via regulation of cap-dependent translation post-radiation (23).

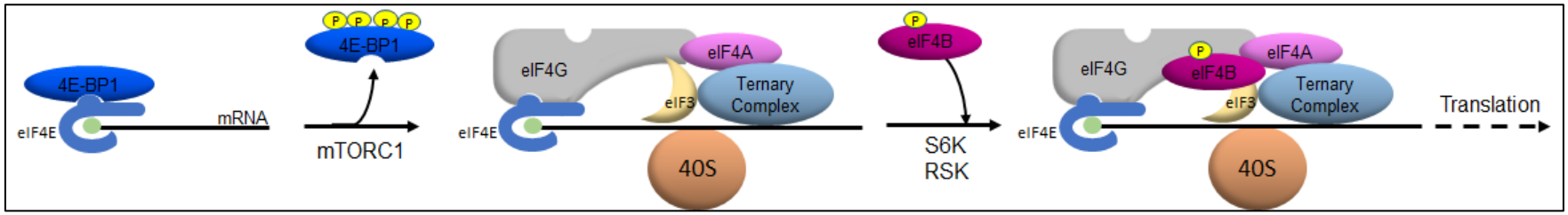

Figure 3: Cap-Dependent Translation Regulation

Eukaryotic translation initiation factor 4E (eIF4E) binds to the 5'-cap of mRNA. In response to growth factors, hyperphosphorylation of inhibitory 4E-binding protein 1 (4E-BP1) mTORC1 allows the recruitment of translation initiation factors eIF4G, eIF4A, and ribosomal 40S subunit to the pre-initiation complex. Ribosomal S6 kinase phosphorylation of eIF4B allows binding and enhancement of mRNA helicase eIF4A.

1.5 OVERVIEW

Protein synthesis is directly correlated with MHC-1 antigen presentation where ~1% of newly synthesized polypeptides are trafficked into the endoplasmic reticulum by transporter associated with antigen presentation (TAP) and loaded onto MHC-1 (21,23,27). Following radiation, antigen presentation results from the degradation of the damaged proteins (23,24). Subsequent DNA damage ATM signaling halts cap-dependent translation via inhibition of mTOR thereby promoting translation of select repair and survival proteins (23,24). After recovery, there is a burst of mTOR-dependent translation to replace damaged proteins (23,24,26). The role of ATR in the regulation of translation has not been explored. Furthermore, the impact of ATM and ATR inhibitors on MHC-1 antigen presentation has not been investigated.

Peptides presented by MHC-1 provide the "self-recognition" signal to cytotoxic T-lymphocytes. In the context of cancer, peptides from mutant proteins are called "neo-antigens" (23,24,27,30). Increased presentation of neo-antigens on the cell surface by MHC-1 has been implicated in increasing the immunogenicity of tumor cells (27-30). Our **objective** is to determine the impact of ATM and ATR kinase inhibitors on MHC-1 antigen presentation in lung cancer. Our **rationale** is that ATR or ATM inhibition increasing the rate of MHC-1 presentation in irradiated lung tumors will improve anti-tumor immune response. We **hypothesize** that ATM and ATR inhibitors disrupt the inhibitory regulation of protein translation impact MHC-1 presentation and potentially the frequency of neo-antigens after ionizing radiation.

2.0 MATERIALS AND METHODS

2.1 TAP1-mNEONGREEN CLONING

A mammalian expression vector was generated to express human spliced variant 1 of Transporter associated with Antigen Processing subunit one (TAP1) with C-terminal monomeric fluorophore NeonGreen (*B. lanceolatum*)(20-22). Simon Watkins, PhD. of the Center for Biological Imaging at the University of Pittsburgh provided an aliquot of the mNeonGreen-N1 mammalian expression vector. pcDNA3.1-TAP1-GFP expression vector was purchased from GenScript. Utilizing unique BamHI and EcoI restriction enzyme sites, the TAP1 gene was amplified by PCR and inserted into the mNeonGreen-N1 vector to generate the TAP1-mNeonGreen vecto

2.2 TAP1-mNEONGREEN U2OS STABLE LINE GENERATION

The TAP1-mNeonGreen vector provides neomycin resistance in positive cells for selection. Osteosarcoma U2OS cells in RPMI supplemented with 10% fetal bovine serum and 5% penicillin streptomycin were transiently transfected with Lipofectamine2000 (ThermoFisher) in a 1:5 DNA to lipid ratio. Transfection of 2ug pEYFP was used as a positive control for of 2ug of TAP1-mNeonGreen transfection. 48hr post-transfection EYFP and TAP1-mNeonGreen expression was confirmed via standard fluorescence microscopy. Growth media was exchanged for selection media containing 500ug/mL G418 (Invitrogen) refreshed at 24hrs and every subsequent 48hrs with replating as necessary (6). Upon elimination of the non-transfected control population, limited dilution cloning of the TAP1-mNeonGreen positive cell population was used to isolate stable line with a medium TAP1-NeonGreen fluorescent phenotype for experimentation.

2.3 FLUORESCENCE RECOVERY AFTER PHOTOBLEACHING OVERVIEW

Fluorescence Recovery After Photobleaching (FRAP) is a method to quantify the mobile fraction and the rate of mobility of molecules within a cellular region (21-23). The molecule of interest is fluorescently tagged (e.g. TAP1-mNeonGreen) and using a high-powered laser a small region of interest is irreversibly photo-bleached. Diffusion of mobile non-bleached molecules from the surrounding area leads to a recovery of fluorescence intensity within the region of interest (21-23). **Figure 4** demonstrates a typical TAP1-mNeonGreen FRAP experiment. Initial fluorescence intensity (Fi) of the region of interest is measured before photobleaching decreases the fluorescence intensity to the minimum (Fo). Over time fluorescence intensity is recovered by the diffusion of non-bleached TAP1-mNeonGreen molecules (mobile fraction). The time required to reach half the maximum recovery(Fmax) is the τ_D. The difference between the maximum fluorescence recovery (Fmax) and the initial fluorescence (Fi) is the immobile fraction of bleached TAP1-NeonGreen molecules within the region of interest. Unidirectional flow within a two-dimensional system, such as a membrane, is due to Brownian motion and can be calculated $D=\omega^2\gamma/4\tau_D$**,** where ω^2 is the area of ROI and γ is the bleaching correction dependent on the laser profile (21-23).

2.4 TAP1-mNEONGREEN LIVE CELL FRAP IMAGING

Confocal analysis of living cells was performed with a Nikon Spectral A1 microscope with a live cell environmental chamber set at 37ºC with constant CO_2 exposure. TAP-mNeonGreen U2OS stable cells were plated on MatTek confocal plates for ~50% density at 24hr prior to imaging. Cells were treated at the indicated times with KU33599 (10uM), CHX (200uM), MG132 (10uM) or DMSO vehicle (0.1%) immediately prior to 2Gy or 5Gy radiation in a ^{137}Cs irradiator. 30minutes post treatment the endoplasmic reticulum was bleached via spot stimulation for 15s with a 488nm laser (75output, 60x objective, 1.4NA, 500Hz, HV(G) 80, 39.6um pinhole, 1/6FPS). Imaging with continuous acquisition for 5min post photobleaching measured the fluorescence recovery within the region of interest.

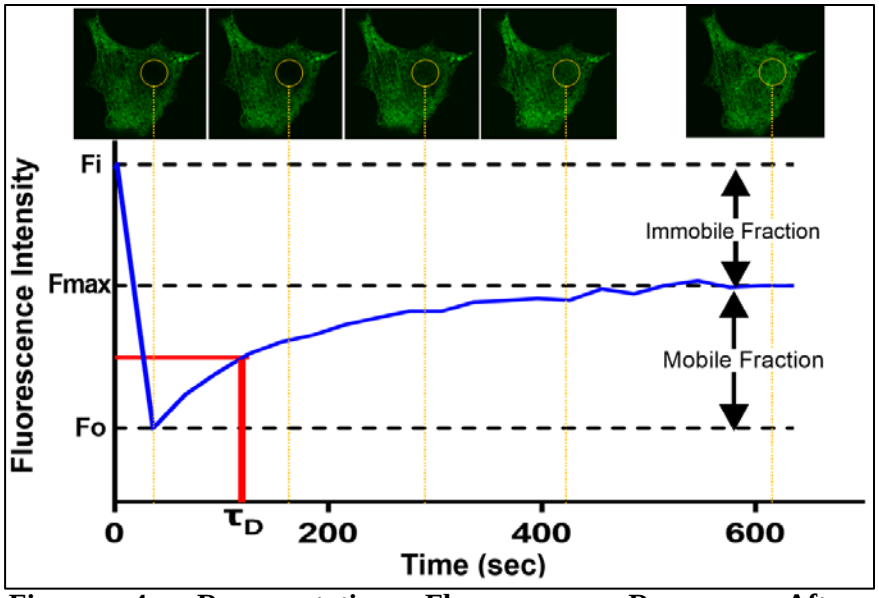

Figure 4: Representative Fluorescence Recovery After Photobleaching (FRAP)

Live-cell TAP1-NeonGreen U2OS stable cell imaging performed with a Nikon A1 Spectral Confocal microscope. Region of Interest (ROI) was bleached with 488nm laser for 30s (75output, 500Hz, 1.4NA, 39.6um pinhole,1/6FPS) and imaged every 15s for 5mins to capture recovery.

2.5 DIFFUSION COEFICIENT DATA ANALYSIS

NIS-Elements4.0 software monitored the fluorescence intensity over time within the defined region of interest while imaging. Post-data acquisition, the time of photobleaching was defined for the NIS-Elements4.0 FRAP analysis software to calculate the rate of recovery (τ_D). To account for differences in ROI area, the lateral diffusion coefficient (D) for each cell was calculated independently as $D=\omega^2\gamma/4\tau_D$**,** where ω^2 is the area of ROI and γ is the bleaching correction (21-23). The average diffusion coefficient of at least 30 technical replicates for each treatment condition from three biological replicates was calculated and depicted as a mean +/- s.d. Statistical significance was determined using GraphPad Prism 7 by ANOVA with Tukey's multiple comparison tests (95% confidence interval).

2.6 ANALYSIS OF MHC-1 CELL SURFACE PRESENTATION BY FLOW CYTOMETRY

A549 and H460 lung adenocarcinoma cells were treated with AZD6738 (10uM or 1uM), or DMSO vehicle (0.1%) at the indicated times with respect to 2Gy radiation in a ^{137}Cs irradiator. Treatment with MG132 (10uM) and CHX (200uM) was performed in the final 4hr of the treatment period. Cells were harvested for MHC-1 surface presentation at 4, 24, or 48hr post treatment in RPMI/10%FBS/5%PenStrep or DMEM/10%FBS/5%PenStrep, respectively. Cell pellets collected via centrifugation at 1,200xg for 5mins were washed 2x with FACS buffer (1xPBS+2%FBS). For surface MHC-1 presentation, live cells were stained in the dark for 30mins at 4^{o} with a mouse FITC-conjugated anti-HuHLA-I (Invitrogen) at 1:300 or mouse anti-IgG2a isotype control (Pierce) at 1:100 antibodies at in FACS buffer. Cells were washed 3x in FACS buffer. Flow cytometry analysis was performed with the Accuri C6 cytometer (BD Biosciences) equipped with the CFlow software to analyze 533/30nm fluorescence intensity of 50,000cells under a medium flow rate (35uL/min). Utilizing scatter (SSC-A vs. FSC-A) gating and fluorescence intensity (SSC-A vs. FL1), the percentage of cells expressing surface MHC-1 above the isotype background control for each treatment condition was determined. Three biologically independent replicates were carried out for each treatment condition and depicted as mean fold increase +/- s.d.. Statistical significance was determined using GraphPad Prism 7 by ANOVA with Tukey's multiple comparison tests (95% confidence interval).

3.0 RESULTS AND ANALYSIS

3.1 MONTORING MHC-1 PEPTIDE LOADING VIA FRAP ANALYSIS OF TAP1-mNEONGREEN

TAP1 is subunit one of transporter associated with antigen processing (TAP) located within the endoplasmic reticulum. TAP is responsible for the transport of peptides from the cytosol into the ER lumen. The MHC-1 peptide loading complex is formed by the interaction of active TAP, unfolded MHC-1, and chaperone proteins tapasin, calreticulin, and ERp57. TAP activity requires an independent ATP conformational change which induces the formation of the active peptide loading complex (27-29). Peptide loading is the rate limiting step to MHC-1 presentation where fluctuations in the size of intracellular antigen pool from alterations in protein translation or degradation effect the activity of TAP and the peptide loading complex (21,23,28). Reits et al. developed a method to indirectly quantify TAP activity via live cell fluorescence recovery after photobleaching (FRAP)(21-23). By tagging the c-terminal tail of TAP1 with a fluorescent fluorophore, mNeonGreen, the 2D lateral diffusion of TAP within the ER membrane can be calculated ($D=\omega^2\gamma/4\tau_D$) from time of half-maximal fluorescence recovery. Active TAP diffuses slower as an open transporter that is associated with the larger peptide loading complex (21,23). Conversely, inactive TAP is closed and unassociated allowing faster diffusion. The diffusion coefficient is inversely proportional to the activity of TAP (21,23).

A spot in the ER of TAP1-mNeonGreen stable U2OS cells was bleached and the recovery of fluorescence intensity overtime was monitored to calculate the diffusion coefficient. To confirm that active translation is required for the activity of TAP, cells were treated with translation inhibitor cycloheximide (CHX) for one hour prior to FRAP experimentation. The diffusion coefficient increased in CHX treated ((1.65e-+/- 0.45) $x10^{-10}$ cm^2s^{-1}) cells compared to the

untreated control ((1.28 +/- 0.51) $x10^{-10}$ cm^2s^{-1}) demonstrating the expected decrease in TAP activity (**Figure 5 left**). Treatment with proteasome inhibitor MG132 should have also increased the diffusion coefficient by decreasing available the peptide pool. Unaccountably, the diffusion coefficient decreased ((1.01 +/- 0.42) $x10^{-10}$ cm^2s^{-1}) compared to the untreated control suggesting increased TAP activity (**Figure 5 left**). Ionizing radiation damages both protein and DNA which disrupts translation both at the ribosomal level and the transcriptional level. To recapitulate the results of Reits et al. (2006) the effects of 5Gy radiation on TAP activity was measured at 1, 2, and 4hrs post irradiation. The diffusion coefficient was significantly increased in the case of a 4hr treatment period with 5Gy ((1.71e-+/- 0.57) $x10^{-10}$ cm^2s^{-1}) demonstrating the expected decrease in TAP activity (**Figure 5 left**).

ATM kinase activity in response to DNA damage has been implicated in contributing to the regulation of cap-dependent translation post ionizing radiation via the mTOR activity (Reits et al 2006). ATM inhibition should prevent the downregulation of translation post radiation thereby increasing the intracellular peptide pool. To evaluate the effects of ATM inhibition, cells were treated with ATM inhibitor Ku55933 prior to radiation with physiologically relevant 2Gy and 5Gy as previously. The diffusion coefficient increased significantly from untreated ((1.3 +/- 0.53) $x10^{-10}$ cm^2s^{-1}) to 2Gy irradiated ((1.78e-+/- 0.79) $x10^{-10}$ cm^2s^{-1}) indicating a decrease in TAP activity (**Figure 5 right**). Contrary to expectation, ATM inhibition alone increased the diffusion coefficient ((1.74e-+/- 0.85) $x10^{-10}$ cm^2s^{-1}) demonstrating decreased TAP activity and non-significantly decreased the effect of radiation when in combination ((1.64e-+/- 0.60) $x10^{-10}$ cm^2s^{-1}) (**Figure 5 right**). The combination of ATM inhibition with radiation was similarly ineffectual with 5Gy ((1.70e-+/- 0.57) $x10^{-10}$ cm^2s^{-1}) and ((1.96e-+/- 0.76) $x10^{-10}$ cm^2s^{-1}) (**Figure 5 right**). The lack of effect in the combination of Ku55933 and radiation suggests that the dynamic range of this technique is not sufficient for this investigation.

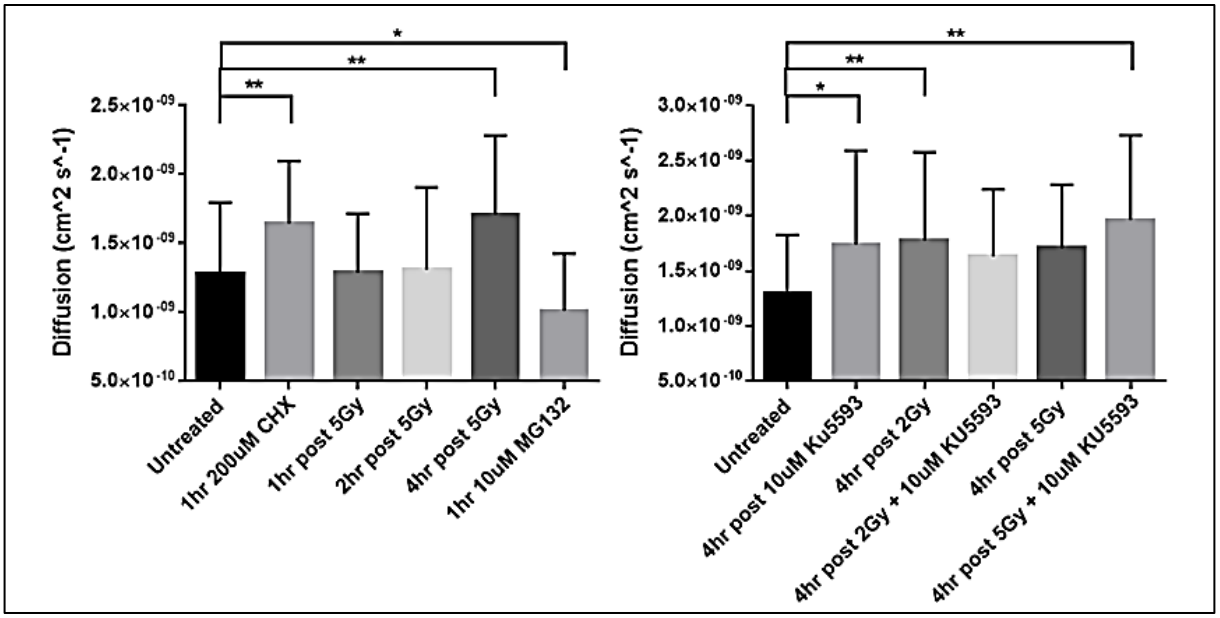

Figure 5: FRAP analysis of TAP1-mNeonGreen U2OS stable cell line.
Live-cell TAP1-NeonGreen U2OS stable cell imaging performed with a Nikon A1 Spectral Confocal microscope. The region of interest (ROI) was bleached with 488nm laser for 30s and imaged every 15s for 5mins to capture recovery. Drugs were administered as indicated and immediately prior to radiation. The 2-dimensional diffusion constant (D) of TAP1 was calculated individually for a minimum of 30 cells. The average D of three independent experiments were plotted with standard deviation. Statistical significance was determined by ANOVA with Tukey's multiple comparison tests (95% confidence interval).

3.2 QUANTIFICATION OF MHC-1 SURFACE EXPRESSION AFTER IONIZING RADIATION

MHC-1 molecules present intracellular antigens to CD8+ cells at the cell surface for self-recognition (27-30). The intracellular antigens are provided by the degradation of nascent peptides and represent the population of proteins being translated within the cell(27-30). Presentation of viral protein antigens or unrecognizable 'neo-antigens' (i.e. heavily mutated or ligated peptides) of cancer cells induce a cytotoxic T lymphocyte response resulting in the clearance of compromised cells (27-30). The landscape of antigen presentation available for CD8+ interactions is dependent on the expression of MHC-1 to the cell surface(27-30).

The effects of DNA-damage response translation regulation post-radiation on of MHC-1 surface presentation were investigated via flow cytometry. For relevance to NSCLC, lung adenocarcinoma cell line A549 was irradiated with physiologically relevant 2Gy radiation after treatment with translation inhibitor CHX, proteasomal inhibitor MG132, ATR inhibitor AZD6738, or ATM inhibitor AZD0156 for 4, 24, and 48hr prior to flow analysis with FITC conjugated anti-HLA-I (MHC-1) antibody. Due to the toxicity of CHX and MG132 treatment with these agents were limited to 4hr treatments periods prior to flow cytometry analysis. The fold change in mean fluorescence intensity for 50,000 cells under each treatment was calculated with respect to the untreated control and depicted as a mean of three independent experiments. At 4hrs post treatment there was no significant difference between the untreated control for any treatment group suggesting that this is too early of a time point to capture a shift in surface expression (**Figure 6 left**). At 24hrs post treatment there are no significant differences, but there is a clear trend of decreased expression with the inhibition of translation (CHX) and proteasomal degradation (MG132) which both decrease the available antigen pool for MHC-1 loading (**Figure 6 middle**). Conversely, radiation and treatment with ATR inhibitor (AZD6738) increased MHC-1 surface expression (**Figure 6 middle**). At 48hrs, there was a 2.2-fold increase in MHC-1 surface presentation with ATR inhibition compared to the untreated control (**Figure 6 middle and right**). Under 2Gy radiation there is a non-significant increase over the untreated control; however, there is a non-significant increase from radiation alone to radiation in combination with ATR inhibition (1.44 vs. 1.87-fold change from untreated) (**Figure 6 middle graph**). The increase with radiation is most likely an increase in degradation proteins damaged by radiation. The increase with ATR inhibition alone suggests that DNA damage response signaling does contribute to protein translation or degradation. The increase in MHC-1 presentation from radiation alone to radiation in combination with ATR inhibition suggests that ATR does effect protein translation or degradation after ionizing radiation. However, there is no indication that the combined effect is not just a result of ATR inhibition alone.

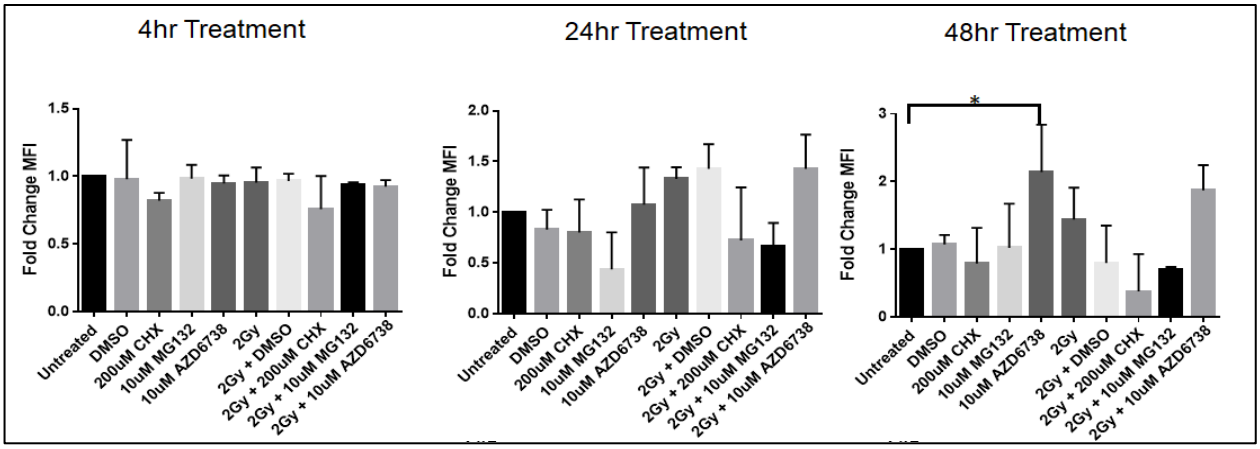

Figure 6: MHC-1 Cell Surface Expression of A549 cells

MHC-1 surface expression of A549 lung adenocarcinoma cells treated with the indicated drug and IR concentrations were analyzed via flow cytometry 4, 24, and 48hr post treatment. 50,000 cells per treatment group were analyzed in three independent experiments. The mean fold change in fluorescence intensity over the untreated control is depicted with standard deviation. Statistical significance was determined by ANOVA with Tukey's multiple comparison tests (95% confidence interval).

4.0 DISUCSSION

4.1 PITFALLS AND IMPROVEMENTS TO TAP1-mNEONGREEN FRAP EXPERIMENTATION

Reits et al. (2000) developed a FRAP method to measure TAP mobility within the ER membrane as an indirect measurement of TAP activity and subsequent MHC-1 presentation. This method was adopted to indirectly investigate alterations in translation and MHC-1 loading by DNA-damage response signaling post ionizing radiation. U2OS stable cells expressing TAP1 c-terminally labeled with the monomeric fluorophore mNeonGreen were generated for FRAP experimentation. Initial control FRAP experimentation with translation inhibitor CHX indicated that there was a significant dynamic range to measure TAP activity with an increase in diffusion coefficient demonstrating decreased TAP activity (**Figure 5 left**). The lack of similar effect from proteosomal inhibition with MG132 was questionable and is potentially a result of using a different inhibitor. Reits et al. used lactacystin which is irreversible and is proteasome specific compared to the reversible MG132 which also targets calpain. They demonstrated that ATP depletion decreased TAP activity as a negative control while micro-injection of small peptides increased TAP activity as a positive control (21,23). Any further utilization of this technique would benefit from recapitulating these controls in conjunction with the CHX and proteasome inhibition negative controls.

Reits et al. (2006) observed a saturation of TAP activity that 1hr after radiation with 1, 7, and 25Gy which lasted longer in a dose dependent manner. In this investigation, 5Gy and physiologically relevant 2Gy produced a significant decrease in TAP activity after 4hrs of treatment period. A similar decrease in TAP activity was observed with ATM inhibition alone

which was unexpected. If ATM activity negatively regulates cap-dependent translation via the inhibition of mTOR in response to genome instability, it would be expected that ATM inhibition will have little or increased TAP activity demonstrated as a decrease the diffusion constant. The unexpected increase in diffusion with Ku55933 inhibition alone is most likely not off target effects as inhibition of mTOR should have a similar effect. This data suggests that ATM is positively regulating translation in the absence of radiation. In combination with radiation; however, the lack of effect may suggest that ATM regulation of translation is independent of signaling activated by ionizing radiation, or more likely that this technique is not robust enough for this purpose. This methodology provides a 'macro' analysis of lateral diffusion of TAP1 which reduces the sensitivity of the technique. The data acquired could be reanalyzed to look at changes in the size of the immobile fraction under different treatment conditions. Alterations in the immobile fraction would inform what fraction of TAP1 molecules within the region of interest are anchored as part of the MHC-1 peptide loading complex as opposed to measuring changes in the moving population.

Variability that could contribute to the lack of sensitivity of the current analysis can stem from issues inherent in live cell FRAP experimentation. The NIS-Elements4.0 software FRAP analysis is not capable of tracking a region of interest as the cell moves during image acquisition. As unbleached regions move in and out of the user designated region of interest fluctuations in the measurement of fluorescence intensity are introduced. To compensate moderate to large technical replicates (i.e. 30+ cells per treatment) are used. Additionally, it is difficult to maintain a standard size for the region of interest. During the photobleaching, the cell moves creating a larger region of interest that is unique to each cell. To compensate the calculation for the diffusion coefficient takes the area variation into account.

In addition to typical live cell imaging pitfalls, the issue of TAP overexpression may contribute to unexpected results. In this investigation, overexpression TAP1-mNeonGreen which has a high potential of disrupting ER activity and the formation of functional TAP heterodimers of TAP1 and TAP2 subunits. An obvious improvement to this model is to introduce the mNeonGreen into the genome c-terminally to TAP1 via CRISPR/Cas9 genome editing(3). Other significant technical improvements would include co-localization data of mNeonGreen with an ER stain. In addition, the comparison of TAP1-mNeonGreen and TAP2-mNeonGreen to demonstrate that there is no subunit dependent functional difference that could contribute mechanistic alterations.

4.2 ATR INHIBITION IMPACT ON MHC-1 CELL SURFACE EXPRESSION

Immune evasion is one of the hallmarks of cancer where tumor cells down regulate immune activating stimuli while up regulating immune deactivating stimuli (19). Current immunotherapy initiatives that target immune deactivating receptors (e.g. PD-L1 and B7) and have proven to be successful in NSCLC suggesting that treatment options that increase immune activating stimuli may improve tumor clearance. MHC-1 molecules presenting unrecognizable antigens, or 'neo-antigens', can trigger the cytotoxic T lymphocyte response against tumor cells (27,30). The pool of antigens available for MHC-1 presentation to CD8+ T cells is dependent translation. Ionizing radiation disrupts translation via short term effects on the protein population and long term via genome instability (23). Inhibition of the DNA-damage response activated by radiation may disrupt translation inhibition post-radiation. Impeding negative regulation of translation during cell recovery could affect the rate MHC-1 presentation recovery after radiation and increase the percentage of 'neo-antigens' presented.

In this investigation, inhibition of translation (CHX) and proteasomal degradation (MG132) for 4hrs induced a non-significant decrease in MHC-1 expression (**Figure 6**). The short treatment time was a compensation for cytotoxicity, longer incubations as lower concentrations would most likely result in a significant decrease in expression. Radiation alone produced a non-significant increase in expression at 48hrs (**Figure 6 right**). Interestingly, ATR inhibition induced a significant increase in expression alone at 48hrs suggesting that the DNA-damage response and ATR specifically is involved in the negative regulation of translation (**Figure 6 right**). ATR inhibition non-significantly increased MCH-1 presentation in combination with radiation suggesting that improved immune recognition could contribute to the efficacy of the combinational therapy. A significant improvement to these experiments would be repeating with a lower concentration of ATR inhibitor closer to the IC50 of the compound.

5.0 FUTURE DIRECTIONS

5.1 TMT-SILAC HYPERPLEXING AS AN ALTERNATIVE TO TAP1-mNEONGREEN FRAP EXPERIMENTATION

In our investigation the intended objective of the TAP1-mNeonGreen FRAP experimentation was to determine if post-ionizing radiation the DNA-damage response signaling negatively regulates translation. The rate of translation is known to directly correlate to the rate of MHC-1 loading and subsequent surface presentation. Inhibition of the DNA- damage response negative translation regulation could potentially increase MHC-1 surface presentation post radiation. FRAP analysis of TAP1-mNeonGreen provided an indirect method to monitor translation as a measurement of intracellular peptide transportation by TAP.

In the interest of a more sensitive, direct quantitative approach, the mass spectrophotometry method TMT-SILAC hyperplexing was explored as an alternative technique to measure the impact of post-radiation DNA-damage response signaling on translation (52). **Figure 7** depicts the simplified work flow for a TMT-SILAC hyperplexeing experiment. 2D cell lines are cultured in the appropriate unlabeled growth medium supplemented with standard antibiotics and dialyzed fetal bovine serum to reduce small molecule background (e.g. amino acids, hormones, or cytokines) present in the serum (52). To quantify the rate of translation, nascent peptides are labeled with heavy ($^{15}N/^{13}C$) L-lysine and L-arginine amino acids in a stable-isotope labeling in cell (SILAC) pulse (52). Cells are split into two populations, unlabeled and SILAC labeled, and treated with ATR inhibitor (AZD6738), ATM inhibitor (AZD0156),
translation inhibitor (CHX), or vehicle control in combination with 2Gy ionizing radiation (Figure 9 for schematic). For this investigation, the plating density for lung adenocarcinoma cell line H460 was optimized to $3x10^5$ cell/mL, $1.5x10^5$cell/mL, or $0.5x10^5$cell/mL to provided approximate cell

population at 24, 48, or 72hr timepoints (**Figure 9**). At various timepoints post SILAC-pulse and treatment, cells are harvested and lysed to generate high-quality peptides for mass spectrophotometry (52). Peptides from each timepoint per treatment group are then labeled with individual tandem mass tags (TMT) identifiers. TMT labeled timepoints for each treatment group are combined into one sample (52). The final sample provides a survey of the proteome of the cell under each treatment condition overtime. Subsequent tandem mass spectrophotometry (LC-MS/MS) provides a readout for the time-resolved SILAC experiments which can be analyzed for the kinetics of translation (52). The increase in $^{15}N/^{13}C$ labeled lysine and arginine incorporation over time (identified by TMT label) provides a quantitative measure of translation (**Figure 7**) (52). In contrast, the decrease in unlabeled peptides over time (identified by TMT label) provides a quantitative measure of protein degradation (**Figure 7**) (52).

TMT-SILAC hyperplexing is a technique that can be utilized to survey the impact of DNA-damage response inhibition on the proteome during cell recovery post-radiation. It is a direct measurement of both the level of translation and what is being translated under different treatment conditions. As a mass spectrophotometry technique, it is also possible to track the translation of a protein under varying treatment conditions. Overall, the TMT-SILAC hyperplexing technique provides a highly sensitive and quantitative method to determine whether inhibition DNA-damage response signaling through ATM and ATR effects translation in the presence or absence of radiation.

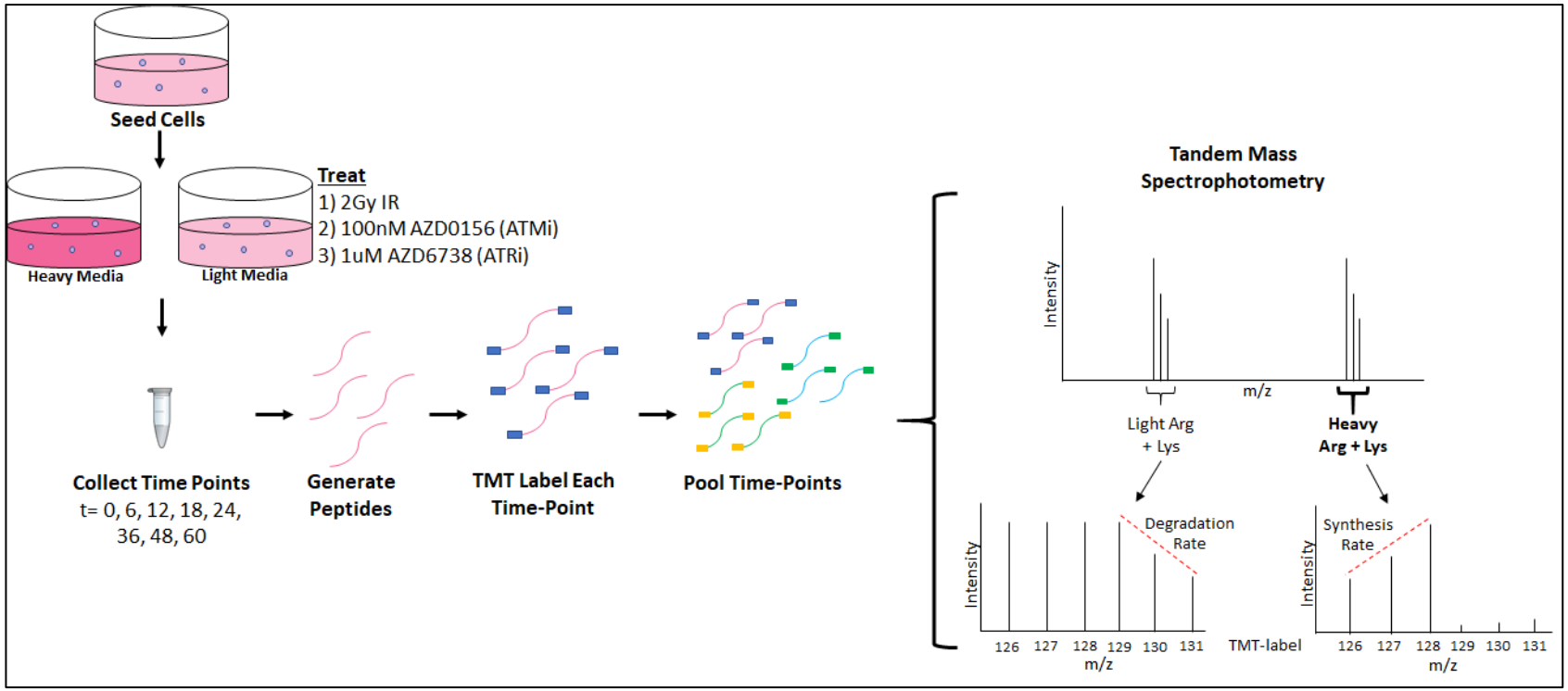

Figure 7: Work flow for TMT-SILAC Hyperplexing

Stable isotope labeling in cells by splitting cell population into two media groups, unlabeled or light media and $^{15}N/^{13}C$ labeled lysine and arginine labeled or 'heavy media'. Plates within each media group are simultaneously treated with compounds and/or radiation. At desired time-points cells are harvested and mass spectrophotometry grade peptides are generated. Peptides are labeled with tandem mass tags (TMT). Each timepoint for each drug treatment are pooled together for tandem mass spectrophotometry. The kinetics of translation are calculated from the increase in 'heavy' of labeled peptides over time. The kinetics of protein degradation are calculated from the decrease in unlabeled peptides over time.

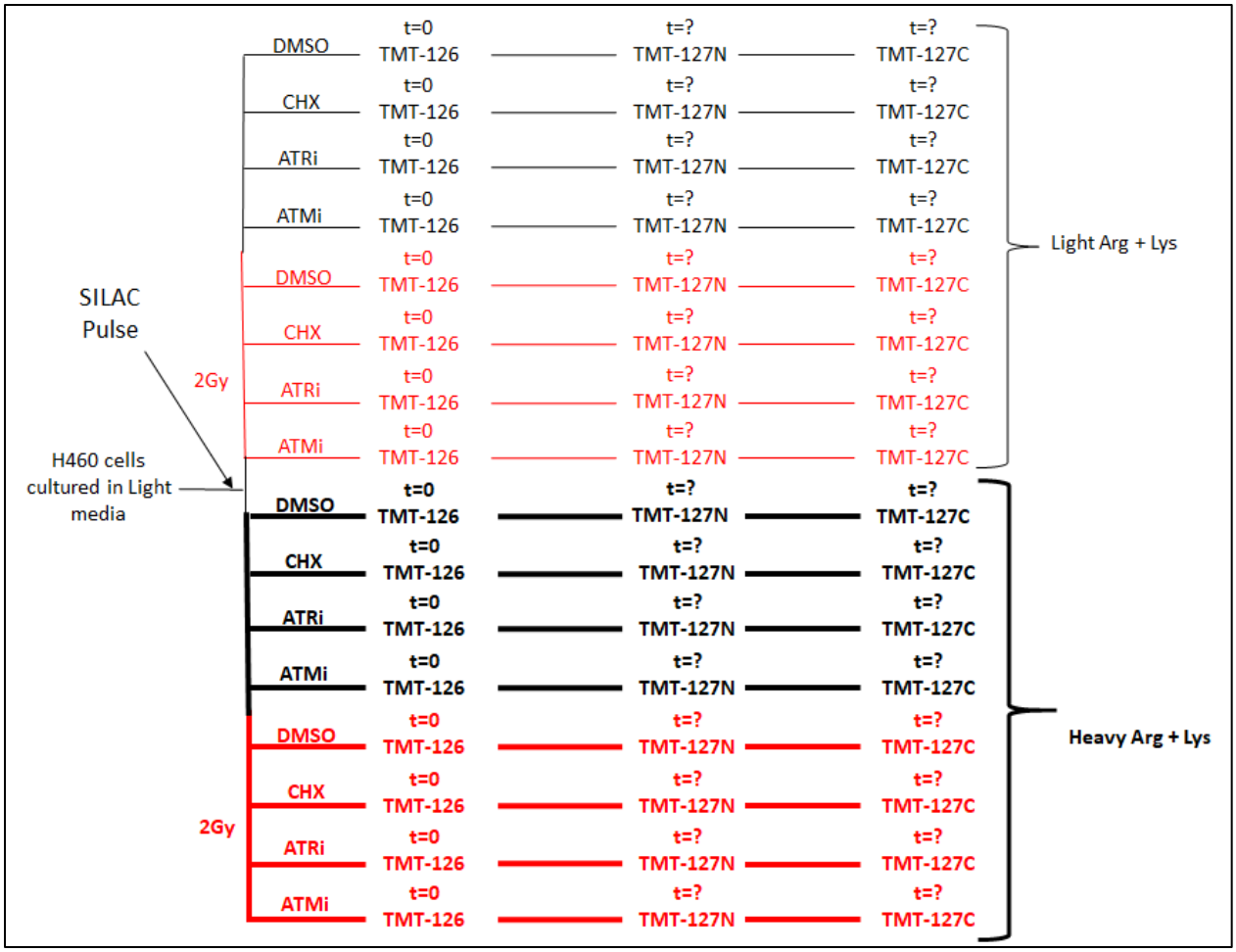

Figure 8: Experimental Schematic for TMT-SILAC Hyperplexing

To survey impact of DNA-damage response inhibition on the level and population of protein translation after radiation sixteen treatment groups will be analyzed. The eight treatment groups per media condition are further split into four drug treatments for irradiated and non-irradiated cells. Drug treaments are as follows: DMSO as the vehicle control, CHX as the positive control for translation inhibition, and AZD6738 or AZD0156 to inhibit ATR and ATM respectively. Peptides for each timepoint are labeled with unique TMT label for identification in LC-MS/MS analysis.

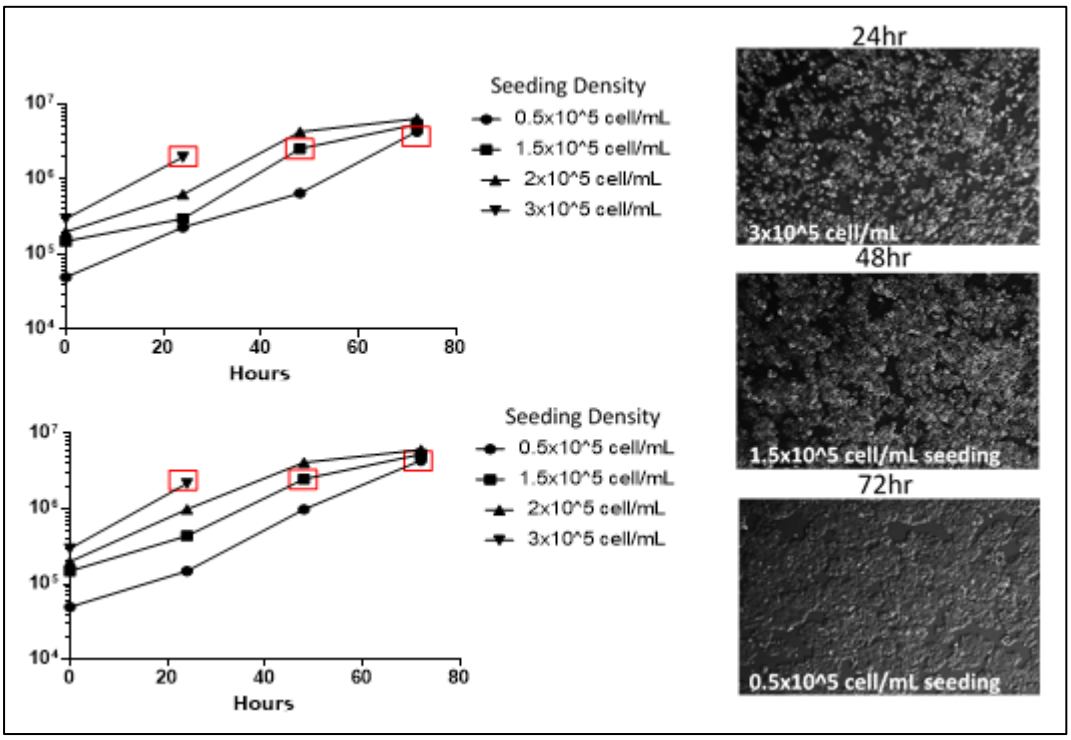

Figure 9: Optimization of H460 Sub-culturing for TMT-SILAC Hyperplexing
Lung adenocarcinoma H460 cell line was cultured in 15cm tissue culture dishes at $8.4x10^4$cells/mL seeding density for 80-90% confluency every 48hr. The number of cells in a single 15cm dish as 80-90% confluency was counted using the Millipore Cell Counter (60um filter) and plated in 10cm dishes at $0.5x10^5$cell/mL, $1.5x10^5$cell/mL, $2x10^5$cell/mL, and $3x10^5$cell/mL. At 24, 48, and 72 hours post-plating, cells were imaged using standard phase-contrast microscope and counted using the Millipore Cell Counter. Cell growth was graphed for each seeding density to determine which density produced similar cell counts at 24, 48, and 72 hrs. Two biological replications are depicted.

5.2 MECHANISTIC ANALYSIS OF DNA-DAMAGRE REPONSE REGULATION OF TRANSLATION

The current investigation has endeavored to quantify the effect of post-radiation DNA-damage response signaling on translation and subsequent MHC-1 surface presentation. However, the techniques discussed so far do not interrogate the mechanism responsible for any shift in translation. TAP1-mNeonGreen FRAP experimentation and the proposed alternative TMT-SILAC hyperplexing measure fluctuations in the level of translation indirectly or directly, respectively. Flow cytometry analysis of the cell surface MHC-1 presentation measures the end-point of the impact of translation regulation post-radiation.

Western blot analysis of translation initiation proteins is a simple, direct and method to examine the mechanism for how the DNA-damage response kinases ATM and ATR regulate translation. The mechanism should be compared in irradiated and non-irradiated in lung cancer cell lines (A549 and H460) under selective inhibition of ATR (AZD6738), ATM (AZD0156), or mTOR (Rapamycin). Western blot analysis of the phosphorylation of ATM, Chk2, ATR, Chk1, mTOR, and p53 will identify the signaling impact of DNA-damage response inhibition after radiation (12-18). Western blot analysis of the phosphorylation of 4E-BP1, eIF4G, eIF4B, and 40S small ribosomal protein S6 kinases will illustrate the impact of DNA-damage response inhibition on the regulation of translation (25,26). Radiation should increase DNA-damage response phosphorylation (ATM, ATR, Chk1, Chk2, p53) while decreasing translation activating phosphorylation (4E-BP1, eIF4G, eIF4B, S6Ks) and increasing inhibitory phosphorylation (mTOR). If the DNA-damage response regulates translation post-radiation, selective pharmacological inhibition should decrease or rescue the impact of radiation on the translation initiation complex.

APPENDIX

Table 1: Abbreviations

Abbreviation	Definition
DDR	DNA damage response
ATM	Ataxia telangiectasia mutated
ATR	Ataxia telangiectasia mutated-related
DSB	Double strand break
SSB	Single strand break
ssDNA	Single-stranded DNA
HR	Homologous recombination
NHEJ	Non-homologous end joining
NSCLC	Non-small cell lung cancer
FRAP	Fluorescence recovery after photobleaching
TAP	Transporter associated with antigen processing
MHC-1	Major histocompatibility complex class 1
CTL	Cytotoxic T lymphocyte

BIBLIOGRAPHY

1. American Cancer Society. Cancer Statistics Center. http://cancerstatisticscenter.cancer.org January (2017)
2. American Cancer Society: Treating NSCLC https://www.cancer.org/cancer/non-small-cell-lung-cancer/treating/surgery.html (2017)
3. Addgene CRISPR 101: A Desktop Resource (1st Edition) www.addgene.org January, 2016
4. Cancer.Net: Lung Cancer-Non-Small Cell: Treatment Options https://www.cancer.net/cancer-types/lung-cancer-non-small-cell/treatment-options August (2017)
5. Clinical Trials: AZD6738 https://clinicaltrials.gov/ct2/results?term=AZD6738&Search=Search
6. Lonza Cologne, Inc. Guideline for Generation of Stable Cell Line: Technical Reference Guide. (2012)
7. My Cancer Genome: Molecular Profiling of Lung Cacner https://www.mycancergenome.org/content/disease/lung-cancer March (2018)
8. NCI Cancer Types: Lung Cancer https://www.cancer.gov/types/lung/patient/non-small-cell-lung-treatment-pdq (April, 2017)
9. Pfzer Oncology: Lung Cancer Fact Sheet. https://www.pfizer.com/files/news/asco/Lung_Cancer_Fact_Sheet_%205_22_15_FINAL.PDF May, 2015
10. The Human Protein Atlas. Cancer Atlas: WSB1. http://www.proteinatlas.org/ENSG00000109046-WSB1/cancer March (2017)
11. Groenendijk, F.H. Bernars R. Drug Resistance to Targeted Therapies: Déjà vu All Over Again. *Molecular Oncology* **8(6)** 1067-1083 (2014)
12. Sasaki, T. Rodig, S.J., Chirieac, L.R., Janne, P.A. The Biology and Treatment of EML4-ALK Non-Small Cell Lung Cancer *Eur J Cancer* **46(10)** 1773-1780 (2010)
13. Shiloh, Y. and Ziv, Y. The ATM protein kinase: regulating the cellular response to genotoxic stress and more. *Nature Reviews: Molecular Cell Biology* **14**, 197-210 (2013)

14. O'Connor M.J. Targeting the DNA Damage Response in Cancer. *Molecular Cell* **60**, 547-560 (2015)
15. Toledo, L.I, Murga, M., and Fermandez-Capetillo, O. Targeting ATR and Chk1 kinases for cancer treatment: A new model for new (and old) drugs. *Molecular Oncology* **5:4**, 368-373 (2013)
16. Lopez-Contreras, A., Fermandez-Capetillo, O. The ATR barrier to replication-born DNA damage. *DNA Repair (Amst)* 10:9(12), 1249-1255 (2013)
17. Yosef Shiloh. ATM and Related Protein Kinases: Safeguarding Genome Integrity. *Nature Reviews: Cancer*. 3, 155-168 (2003)
18. Benada, J.; Macurek L. Targeting the Checkpoint to Kill Cancer Cells. *Biomolecules* **5**; 1912-1927 (2015)
19. Hanahan,D. Weinberd, R.A. Hallmarks of Cancer: The Next Generation. *Cell* **144** 646-647 (2011)
20. Shaner, N.C., Lambert, G.G., Chammas, A., Ni, Y., Cranfill, P.J., Braid, M.A., Sell, B.R., Allen, J.R., Day, R.N., Israselsson, M., Davidson, M.W., Wang, J. A birght monomeric green fluorescent protein derived from Branchiostoma Ianceolatum. *Nat Methods* **10(5);** 407-409 (2013)
21. Reits, E.A.J., Vos, J.C., Gromme, M,, Neejes, J. The major substrates for TAP in vivo are derived from newly synthesized proteins. *Nature* **404**; 774-778 (2000)
22. Reits, E.A.J., Neefjes, J. From fixed to FRAP: measuring protein mobility and activity in living cells. *Nat Cell Bio: Tech* Rev **3**; E145-E147 (2001)
23. Reits, E.A., Hodge, J.W., Herberts, C.A., Groothuis, T.A., Chakraborty, R.M., Wansley, E.K., Camphausen, K., Luiten, R.M., de Ru, A.H., Neijessen, J., Griekspoor, A., Mesman, E., Verreck, F.A., Spits, H., Schlom, J., van Veelen, P., Neefjes, J.J., Radiation modulates the peptide repertoire, enchances MHC class I expression, and induces successful antitumor immunotherapy. *JEM* **203**; 1259-1271 (2006)
24. Braustein, S., Badura, M.L, Xi, Q., Formenti, S.C., Schneider R.J. Regulation of Protein Synthesis by Ionizing Radiation *Molecular and Cell Biology* **29:21,** 5645-5656 (2009)
25. Haimov, O, Sinvani, H., Dikstein, R. Cap-dependent, scanning-free translation initiation mechanisms. *Biochemica et Biophysica Acta* **1849** 1313-1318(2015)

26. Max Ma, X., Blenis, J. Molecular Mechanisms of mTOR Mediated Translational Control. *Nature Reviews: Molecular Cell Biology* **10** 307-318 (2009)
27. Neefjes, J., Jongsma, M.L.M., Paul, P., Bakke, O. Towards a systems understanding of MHC class I and MHC class II antigen presentation. *Nature Reviews Immunology* **11;** 823-836 (2011)
28. Hughes, E.A., Hammond, C, Cresswell, P. Misfolded Major Histocompatibility Complex Class I Heavy Chains are Translocated into the Cytoplasm and Degraded by the Proteasome. *Proccedins of the Natural. Academy of Science USA* **94** 1896-1901 (1997)
29. Wearcsh, P.A., Cresswell P. The Quality Control of MHC-1 peptide Loading *Curr. Opin. Cell Biology* **20** 624-631(2008)
30. Brown, S.D., Warren, R.L., Gibb, E.A. Martin, S.D., Spinelli, JJ., Nelson, B.H., Holt, R.A. Neo-antigens predicted by tumor genome meta-analysis correlate with increased patient survival. *Genome Research***24**; 743-750 (2014)
31. Ferreara T.A, Hodge, J.W., Gulley, J.L. Combining Radiation and Immunotherapy for Synergistic Anti-tumour Therapy *Currt Opin on Mol Ther* 11, 37-42(2009)
32. Dominques, D, Turner A, Silca MD, Marques DS, Mellidez JC, Wannesson L, Mountzios G, de Mello RA. Immunotherapy and Lung Cancer: Current Developments and Novel Targeted Therapies. *Immunotherapy* **6(11)** 1221-1235 (2014)
33. Anagnostou VK, Brahmer JK. Cancer Immunotherapy: A Future Paradigm Shift in the Treatment of Non-Small Cell Lung Cancer. *Clinical Cancer Research* **21(5)** 976-984 (2015)
34. Cortinovis D, Abbate M, Bidoli P, Capici S, Canova S. Targeted Therapies and Immunotherapy in Non-Small Cell Lung Cancer *eCancer Medical Science* **10** 648 (2016)
35. Vendetti, F.P., Lau, A., Schamus, S., Conrads, T.P., O'Connor, M.J., Bakkenist, C.J. The orally active and bioavailable ATR kinase inhibitor AZD6738 potentials the anti-tumor effects of cisplatin to resolve ATM-deficient non-small cell lung cancer in vivo. *Oncotarget* **(**2015)
36. Toledo, L.I; Murga, M.; Zur, R.; Soria, R.; Rodrigues, A.; Martinez, S.; Oyarzabal, J.; Pastor, J.; Biscoff, J.R.; Fernandez-Capetillo, O. A cell-based screen identifies ATR inhibitors with synthetic lethal properties for cancer-associated mutations. *Nat Struct Mol Bio.* **18:6**;721-727 (2011).

37. Reaper P.M., Griffiths, M.R., Long, J.M., Charrier, J-D., MacCormick, S., Charlton, P.A., Golec, J.M.C., Pollard, J.R. Selective Killing of ATM or p53-Deficient Cancer Cells Through Inhibition of ATR *Nature Chem. Bio. Comm.* **7;** 428-430 (2011)
38. Prevo, R., Fokas, E., Reaper, P.M., Charlton, P.A., Pollard, J.R., McKenna, W.G., Muschel, R.J., Brunner, T.B. The Novel ATR Inhibitor VE-821 Increases Sensitivity of Pancreatic Cancer Cells to Radiation and Chemotherapy *Cancer Biology & Therapy* **13:11,** 1072-1081 (2012)
39. Hall, A.B., Newsome, D., Wang, Y., Boucher, D.M., Eustace, B., Gu, Y., Hare, B., Johnson, M.A., Milton, S., Murphy, C.E., Takemoto, D., Tolman, C., Wood, M., Charlton, P., Charrier, J-D., Furey, B., Golec, J., Reaper, P.M., Pollard, JR. Potentiation of Tumor Responses to DNA Damaging Therapy by the Selective ATR Inhibitor VX-970 *Oncotarget* **5:14**, 5674-5685 (2014)
40. Teng, P.; Bateman, N.W.; Darcy, K.M.; Hamilton, C.A.; Maxwell, G.L.; Bakkenist, C.J.; Conrads, T.P. Pharmacologic inhibition of ATR and ATM offers clinically important distinctions to enhancing platinum or radiation response in ovarian, endometrial, and cervical cancers. *Gynecol Oncol.***136:3**;554-561(2015)
41. Villaruz, L.C., Jones, H., Dacic, S., Abberbock, S., Kurland, B.F., Stabile, L.P., Siegfried, J.M., Conrads, T.P., Smith, N.R., O'Connor, M.J., Pierce, A., Bakkenist, C.J. ATM protein is deficient in over 40% of lung adenocarcinomas. *Oncotarget* (2016)
42. Liu, R., Tang, J., Ding, C., Liang, W., Zhang, L., Chen, T., Xiong, Y., Dai, X., Li, W., Xu, Y., Hu, Jin., Lu, L., Liao, W., and Lu, W. The Depletion of ATM inhibits colon cancer proliferation and migration via B56gama2-mediated Chk1/p53/CD44 Cascades. *Cancer Letters* **390**, 48-57 (2017).
43. Rainey, M.D; Charlton, M.E.; Stanton, R.V.; Kastan, M.B. Transient inhibition of ATM kinases is sufficient to enhance cellular sensitivity to ionizing radiation. *Cancer Research* **68:18**; 7466-7474 (2008)
44. Yamamoto, K.; Wang, Y.; Jiang, W; Dubois, R.L.; Lin, C-S; Ludwig, T.; Bakkenist, CJ; Zha, S. Kinase-dead ATM protein causes genomic instability and early embryonic lethality in mice. *The Journal of Cell Biology* **198:3**; 305-313 (2012)

45. Daniel, J.A., Pellegrini, M., Lee, B-S., Guo, Z., Filsuf, D., Belkina, N.V., You, Z., Paull, T.T., Sleckman, B.P., Feigenbaum, L., Nussenzweig, A. Loss of ATM kinase activity leads to embryonic lethality in mice. Journal of Cell Biology 198:3, 295-304 (2012)
46. Petersen, L.F; Klimowicz, A.C.; Otsuka, S.; Elgbede, A.A.; Petrillo, S.K.; Williamson, T.; Williamson CT.; Konno, M; Lees-Miller, S.P.; Hao, D.; Morris, D.; Magliocco, A.M.; Bebb, D.G. Loss of tumour-specific ATM protein expression is an independent prognostic factor in early resected NSCLC. *Oncotarget* (2017)
47. Beumer, J.H; Fu, K.Y.; Anyang B.N.; Siegfried, J.M.; Bakkenist, C.J. Functional analysis of ATM, ATR, and Facnoci anemia proteins in lung cancer. *BMC Cancer* **15:649** (2015)
48. Weber, A.M; Dorbnitzky, N.; Devery, A.M.; Bokobza, S.; Adams, R.A.; Maughan T.S.; Ryan, A.J. Phenotypic Consequences of somatic mutation in the ataxia-telangiectasia mutated gene in non-small cell lung cancer. Oncotarget (2016)Yang, H.; Spitz, M.R.; Stewar, D.J.; Lu, C.; Gorlov, I.P; Wu, X. ATM sequence variants associate with susceptibility to non-small cell lung cancer. *Int. J Cancer* **121(10):**2254-2259 (2007)
49. Menotta, M.; Biagiotti, S.; Bianchi, M.; Chessa, L.; Magnani, M. Dexamthasone Partially Rescues Ataxia Telangiectasia-mutated (ATM) Deficiency in Ataxia Telangiectasia by Promoting a Phortened PRotien Variant Retaining Kinase Activity. *Journal of Biological Chemistry* **287**(49); 41352-41363 (2012).

50. Ding, L., Getz, G., Wheeler, D. A., Mardis, E. R., McLellan, M. D., Cibulskis, K., Sougnez, C., Greulich, H., Muzny, D. M., Morgan, M. B., Fulton, L., Fulton, R. S., Zhang, Q., Wendl, M. C., Lawrence, M. S., Larson, D. E., Chen, K., Dooling, D. J., Sabo, A., Hawes, A. C., Shen, H., Jhangiani, S. N., Lewis, L. R., Hall, O., Zhu, Y., Mathew, T., Ren, Y., Yao, J., Scherer, S. E., Clerc, K., Metcalf, G. A., Ng, B., Milosavljevic, A., Gonzalez-Garay, M. L., Osborne, J. R., Meyer, R., Shi, X., Tang, Y., Koboldt, D. C., Lin, L., Abbott, R., Miner, T. L., Pohl, C., Fewell, G., Haipek, C., Schmidt, H., Dunford-Shore, B. H., Kraja, A., Crosby, S. D., Sawyer, C. S., Vickery, T., Sander, S., Robinson, J., Winckler, W., Baldwin, J., Chirieac, L. R., Dutt, A., Fennell, T., Hanna, M., Johnson, B. E., Onofrio, R. C., Thomas, R. K., Tonon, G., Weir, B. A., Zhao, X., Ziaugra, L., Zody, M. C., Giordano, T., Orringer, M. B., Roth, J. A., Spitz, M. R., Wistuba, II, Ozenberger, B., Good, P. J., Chang, A. C., Beer, D. G., Watson, M. A., Ladanyi, M., Broderick, S., Yoshizawa, A., Travis, W. D., Pao, W., Province, M.A., Weinstock, G.M., Varmus, H E., Gabriel, S. B., Lander, E. S., Gibbs, R. A., Meyerson, M., and Wilson, R. K. Somatic mutations affect key pathways in lung adenocarcinoma. *Nature* **455**, 1069-1075 (2008)
51. Cancer Genome Atlas Research, N. Comprehensive molecular profiling of lung adenocarcinoma. *Nature* **511**, 543-550 (2014)
52. Welle K.A., Zhang, T., Hyrohorenko, J.R., Shen, S., Qu, J., Gharmmaghami, S. Time-Resolved Analysis of Proteome Dynamics by TMT-SILAC Hyperplexing *Amer Soc Biochem Mol Bio* (2016)